Korean J. Chem. Eng., **22**(3), 441-451 (2005)

Simulation and Analysis of Extractive Distillation Process in a Valve Tray Column Using the Rate Based Model

Sasmita Pradhan and Aravamudan Kannan†

Department of Chemical Engineering, Indian Institute of Technology Madras, Chennai 600 036, India
(*Received 6 September 2004 • accepted 14 February 2005*)

Abstract–Valve trays are becoming popular in the chemical process industries owing to their flexibility to handle a wide range of vapor throughputs. Using the rigorous rate based model, the importance of the non-equilibrium approach is demonstrated for a typical extractive distillation process in a Glitsch V-1 valve tray column. Simulation results based on an in-house developed code indicated that the rate based model predictions for a valve tray column operation showed significant differences relative to the equilibrium model. Even small errors in product purities translated into non-optimal feed stage locations and inaccurate number of stages required. The counter-intuitive effect of high reflux ratio on separation is explained.

Key words: Valve Tray Column, Extractive Distillation, Rate-based Model, Distillation Column Design

INTRODUCTION

A major part of the operations in a chemical process plant is centered on separation processes, which typically include distillation columns, absorbers and extractors. It is essential to ensure accurate design of this equipment, since even a small difference between the separation achieved and target specified may have considerable environmental and economic implications. The present work emphasizes distillation since it is usually the first choice to meet separation requirements.

Conventionally, multistage separation processes were modeled in terms of the equilibrium stage model, which assumes the attainment of thermodynamic equilibrium between the contacting phases. However, multicomponent diffusion phenomena may involve coupling of concentration gradients of different species leading to uncommon behaviour such as reverse diffusion, diffusion barrier, osmotic diffusion etc. [Toor, 1957, 1964]. For systems exhibiting strong thermodynamic non-ideality, the efficiencies could vary significantly and can even lie between $-\infty$ to $+\infty$. Hence, multicomponent Murphree efficiencies and their variation with respect to component as well as stage are difficult to estimate and incorporate into the equilibrium model. The development of the rigorous non-equilibrium or rate based model, described in detail by Taylor and Krishna [1993] obviated the need for use of Murphree efficiencies for multicomponent systems. Briefly, this model considers each phase to be separated by an interface through which heat and mass transfer occur. The transport of mass and heat through both phases implies the existence of concentration and temperature gradients in both phases. While the temperature gradient was continuous across the interface, the concentration at the interface was related by the equilibrium relationship. The MERSQ equations developed for the rate-based model are summarized in Table 1. The equilibrium model equations corresponding to reboiler and condenser are summarized in Table 2. The procedures for estimating the multicomponent mass transfer coefficients using the film theory are summarized in Table 3. The rate based model has been extensively applied in several applications. These are briefly reviewed below.

In one of the earlier studies, Lee et al. [1997] investigated the packed distillation columns with a rate based model. Springer et al. [2002] recommended the model for predicting the distillation boundary crossing characteristics observed in ternary azeotropic distillation processes. Pyhalahti and Jakobsson [2003] developed a rate based mixed pool model and recommended its application for absorbers with high exothermic reactions. Sanpui and Khanna [2003] have investigated the selection of mass transfer correlations for rate based liquid-liquid extraction models. Peng et al. [2003] developed rate based and equilibrium models for the production of tert-amyl methyl ether (TAME) in packed columns using gPROMS software. These authors recommended simplification of the rate based model for model based control. Kloker et al. [2003] studied the influence of operating conditions and column configuration on the performance of reactive distillation columns with liquid-liquid separators. Mortaheb and Kosuge [2004] studied the simulation and optimization of a heterogeneous azeotropic distillation process in a sieve tray column. Hoffman et al. [2004] studied the scale up characteristics of the structured packing, MULTIPAK®, that was applied in methyl acetate synthesis. Kenig et al. [2004] described the features of the advanced rate based simulation tools in reactive distillation that included reaction in the film and catalyst efficiency. Higler et al. [2004] have used the nonequilibrium stage modeling for three phase distillation. First, the equilibrium 2 phase model was solved to generate initial guesses for solving the equilibrium three phase model. These results in turn were used to solve the rigorous three phase rate based model. Noeres et al. [2004] adopted dynamic simulation of catalytic distillation columns in methyl acetate synthesis. For offline and online optimization and control reduced order and simplified models were applied. While the rate based model is rigorous, it can also become difficult to implement for dynamic simulations, optimization and control. Further, the parameters of the model such as the mass transfer coefficients may be difficult to estimate accurately. Equilibrium based models can serve as useful limits to the rate based

†To whom correspondence should be addressed.
E-mail: kannan@iitm.ac.in

Table 1. MERSQ equations for column stages modeled as non-equilibrium stages [Taylor and Krishna, 1993]

Significance	Liquid phase (j^{th} stage, i=1, 2, …, c)	Vapor phase (j^{th} stage, i=1, 2, …, c)	Interface (j^{th} stage i=1, 2, …, c)
Component Material balances (M_{ij}^L and M_{ij}^V)	$(1+r_j^L)L_jx_{ij}-L_{j-1}x_{i,j-1}-f_{ij}^L-N_{ij}^L=0$	$(1+r_j^V)V_jy_{ij}-V_{j+1}y_{i,j+1}-f_{ij}^V-N_{ij}^V=0$	-
Total material balances (M_{tj}^L and M_{tj}^V)	$(1+r_j^L)L_j-L_{j-1}-F_j^L-N_{tj}^L=0$ where $F_j^L=\sum_{i=1}^{c}f_{ij}^L$ and $N_{tj}^L=\sum_{i=1}^{c}N_{ij}^L$	$(1+r_j^V)V_j-V_{j+1}-F_j^V+N_{tj}^V=0$ where $F_j^V=\sum_{i=1}^{c}f_{ij}^V$ and $N_{tj}^V=\sum_{i=1}^{c}N_{ij}^V$	-
Energy balances in the bulk phases (E_j^L and E_j^V)	$(1+r_j^L)L_jH_j^L-L_{j-1}H_{j-1}^L-F_j^LH_j^{LF}+Q_j^L-e_j^L=0$	$(1+r_j^V)V_jH_j^V-V_{j+1}H_{j+1}^V-F_j^VH_j^{VF}+Q_j^V+e_j^V=0$	
Energy balance at the interface (E_j^I)	-	-	$e_j^V-e_j^L=0$ where e_j^V and e_j^L are given by $a_jh_j^V(T_j^V-T_j^I)+\sum_{i=1}^{c}N_{ij}^V\overline{H}_{ij}^V$; $a_jh_j^L(T_j^I-T_j^L)+\sum_{i=1}^{c}N_{ij}^L\overline{H}_{ij}^L$
Rate equations (R_{ij}^L and R_{ij}^V)	$N_{ij}-N_{ij}^L=0$ i=1, 2, …, c−1 where $N_i^L=J_i^L+\overline{x}_iN_t^L$	$N_{ij}-N_{ij}^V=0$ i=1, 2, …, c−1 where $N_i^V=J_i^V+\overline{y}_iN_t^V$	-
Constraint at the interface (S_j^{LI}, S_j^{VI})	-	-	$\sum_{i=1}^{c}x_{ij}^I-1=0$; $\sum_{i=1}^{c}y_{ij}^I-1=0$
Equilibrium relationship (Q_{ij}^I)	-	-	$K_{ij}^Ix_{ij}^I-y_{ij}^I=0$
No. of Equations	2c+1	2c+1	c+3

Table 2. MESH equations for reboiler and condenser modeled as equilibrium stages [Taylor and Krishna, 1993]

Significance	Equation (I=1, 2, …, c)
Component material balances (M_{ij})	$M_{ij}\equiv(1+r_j^V)V_jy_{ij}+(1+r_j^L)L_jx_{ij}-V_{j+1}y_{i,j+1}-L_{j-1}x_{i,j-1}-f_{ij}=0$
Total material balance (M_{tj})	$(1+r_j^V)V_j+(1+r_j^L)L_j-V_{j+1}-L_{j-1}-F_j=0$ where $f_{ij}=f_{ij}^V+f_{ij}^L$ and $F_j=F_j^V+F_j^L$
Energy balance (E_j)	$H_j\equiv(1+r_j^V)V_jH_j^V+(1+r_j^L)L_jH_j^L-V_{j+1}H_{j+1}^V-L_{j-1}H_{j-1}^L-F_jH_j^F+Q_j=0$ where $F_jH_j^F=F_j^VH_j^{VF}+F_j^LH_j^{LF}$ and $Q_j=Q_j^V+Q_j^L$
Mole fraction constraint (S_j)	$\sum_{i=1}^{c}(x_{ij}-y_{ij})=0$
Equilibrium relationship ($E_{i,j}$)	$K_{ij}x_{ij}-y_{ij}=0$
No. of Equations	2c+3

Table 3. Estimation of multi-component mass transfer coefficient matrices in the non-equilibrium model by film theory [Taylor and Krishna, 1993]

Parameter	Equations		
Multicomponent mass transfer coefficient matrices $[k^V]$ and $[k^L]$	$R_{ii}=\frac{m_i}{\kappa_{ic}}+\sum_{\substack{k=1\\k\neq i}}^{c}\frac{m_k}{\kappa_{ik}}$	i=1, 2, … c−1	$(J^V)=[k^V](\overline{y}-y^I)$ and $(J^L)=[k^L](x^I-\overline{x})$ where $[k]=[R]^{-1}[\Gamma]$
	$R_{ij}=-m_i\left(\frac{1}{\kappa_{ij}}-\frac{1}{\kappa_{ic}}\right)$	i=1, 2, … c−1	
	m_i is the mole fraction of appropriate phase and κ_{ij} is the binary mass transfer coefficient		
	For liquid and vapor phases, the thermodynamic correction factors (Γ^L and Γ^V) are given by :		
	$\Gamma_{ij}^L=\delta_{ij}+x_i\left.\frac{\partial\ln\gamma_i}{\partial x_j}\right\vert_{T,P,\Sigma}$	i, j=1, 2, … c−1	
	$\Gamma_{ij}^V=\delta_{ij}+x_i\left.\frac{\partial\ln\varphi_i}{\partial x_j}\right\vert_{T,P,\Sigma}$		

models and have also been used in recent times in the analysis of complex distillation processes for e.g. by Kim et al. [2004] and Assabumrungrat et al. [2004].

SCOPE OF THE CURRENT STUDY

Valve tray distillation columns are considered in this work since

they have significant advantages over conventional sieve trays owing to their high turn down ratio. This gives them the flexibility to handle a wide range of vapor flow rates ranging from a minimum throughput to the normal or design throughput [Kister, 1992]. From the above typical studies it may be noted that valve trays have not been investigated in detail using the rate based model. The simulation studies on the Glitsch V-1 valve tray column are reported in this work. The influence of the mass transfer coefficients on the rate governed separation process is explored in detail. The design implications of the seemingly minor discrepancies that arise between the equilibrium and rate based model predictions are illustrated. Further, the counter-intuitive effect of high reflux ratio on product purity is illustrated. In order to implement the rate based model, an in-house code was developed by using the object-oriented JAVA programming approach.

Table 4. Degrees of freedom analysis for the rate based model equations

Variables		Equations	
Name	No.	Name	No.
y_{ij}, x_{ij}	2c	M_{ij}^{V}, M_{ij}^{L}	2c
V_j, L_j	2	M_{1j}^{V}, M_{1j}^{L}	2
T_j^{V}, T_j^{L}	2	E_j^{V}, E_j^{L}	2
T_j^{I}	1	E_j^{I}	1
y_{ij}^{I}, x_{ij}^{I}	2c	R_{ij}^{V}, R_{ij}^{L}	2(c−1)
N_{ij}	c	S_j^{VI}, S_j^{LI}	2
		Q_{ij}^{I}	c
Sum	5c+5	Sum	5c+5

CASE STUDY

A Glitsch V-1 valve tray column used in the extractive distillation of methanol from its mixture with acetone using water as the solvent was simulated by using the rate based model. A degrees of freedom analysis was performed for the rate based model, and the results are shown in Table 4. The equations in Table 4 correspond to the MERSQ equations listed in Table 1. For the reboiler and condenser the degrees of freedom analysis is much simpler involving (2c+3) variables (y_{1j}, y_{2j}, … y_{cj}, V_j, T_j, x_{1j}, x_{2j}, … x_{cj}, L_j). The corresponding 2c+3 independent MESH equations for an equilibrium stage as described in Table 2 are (M_{1j}, M_{2j}, … M_{cj}, M_{ij}, H_j, E_{1j}, E_{2j}, … E_{cj}, S_j). The specifications of a typical column simulation are presented in Table 5. The schematic sketch of the extractive distillation column is given in Fig. 1. Zone 1 refers to the section above the solvent entry, zone 2 refers to the section of column between the two feeds and zone 3 refers to the section below the second feed.

1. Properties Estimation

The reliability of the simulation results depends to a large extent on the accuracy with which the properties and transfer coefficients are estimated. The property models used in this work are given in Table 6. The predicted properties compared satisfactorily with the predictions of Aspen Plus® software over a wide range of compositions and temperatures. The gas and liquid mass transfer coeffi-

Table 5. Specifications for simulation

Specifications		Typical Case Study
Number of stages (including condenser and reboiler)		20
Condenser		Partial (equilibrium stage)
Reboiler		Partial (equilibrium stage)
Tray type		Glitsch V-1 valve
Column diameter, m		1.83
Exit weir height, m		0.05715
Bubbling (active) area, m^2		2.1064
Reflux ratio		4
Bottom rate		68.774 mol/s
Flow type		Mixed for both vapour and liquid
Pressure		Top stage : 101.3 kPa Bottom stage : 116.84 kPa Intermediate stages : linear pressure profile between top and bottom stage pressure
Feed 1 (Solvent : Water)	Location	stage 3
	State, T&P	liquid at 323 K, 103.33 kPa
	Flow rates	Acetone 0.0 mol/s Methanol 0.0 mol/s Water 60 mol/s
Feed 2 Acetone-Methanol Mixture	Location	stage 10
	State, T&P	bubble point liquid (330.48 K), 108.39 kPa
	Flow rates	Acetone 30 mol/s Methanol 10 mol/s Water 0 mol/s

cients and interfacial area for Glitsch V-1 valve trays were obtained from the correlations developed by Sheffe and Weiland [1987].

2. Details of Simulation

Fig. 2 shows the object oriented representation of the simulation organization using the convention suggested by Rumbaugh et al. [1993]. The features of the object oriented approach are data encapsulation, modular code development and inheritance of classes, thereby enabling more flexibility, extensibility and easier maintenance of the code. An aggregation of components classes forms the stream class, several of which are associated with the stage class. In turn, an aggregation of stages forms the column class from which specific classes such as distillation and absorption columns are inherited. From property estimation and numerical computation viewpoints, the property and matrix classes are also associated as shown. The following steps are involved in the simulation.

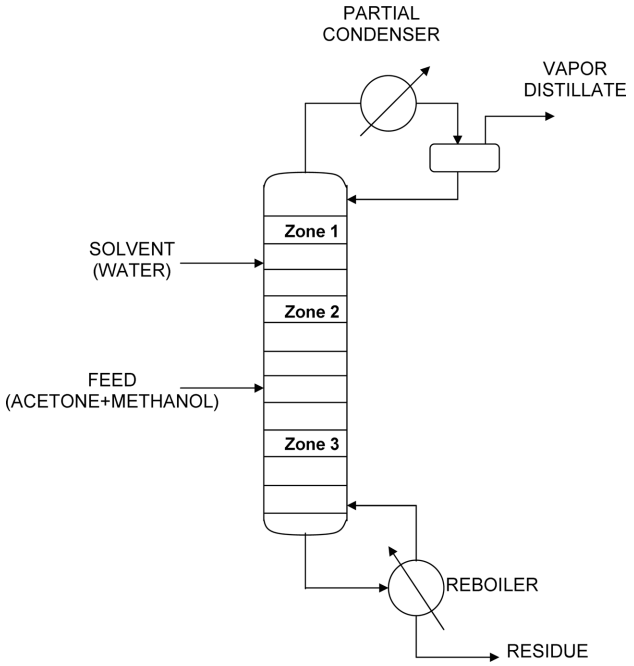

Fig. 1. Schematic diagram of extractive distillation for acetone-methanol-water system.

i. The column operating conditions such as reflux ratio, distillate, solvent and feed flow rates, side stream flow rates (if any) as well as the design parameters such as tower diameter, type of condenser and reboiler, number of stages, active area and weir height are specified.

ii. The property data base of the system used in the simulation is initialized with appropriate parameters.

iii. A new distillation class instance - the distillation object is created.

iv. The data in (i) are assigned to the streams, stages and tray dimensions using appropriate functions.

v. The simulation function of the distillation object is executed.

vi. Initial guesses are generated.

vii. The column equations (in Tables 1 and 2) are solved by using the appropriate matrix routines and results are displayed.

The model equations (discrepancy functions) and unknown variables were grouped stagewise and solved simultaneously by the usual Newton-Raphson iterative scheme. Suitable initial guesses

Table 6. Property Models used in this study [Reid et al., 1988]

Properties	Models
Vapour-liquid equilibrium ratio (K)	Modified Raoult's law
Activity coefficients	UNIFAC
Fugacity coefficients	Equation of State (Redlich-Kwong)
Enthalpy	Ideal (for vapour phase)
	Ideal+excess enthalpy (for liquid phase from activity coefficient models)
Enthalpy of vapourization	Watson's model
Vapour pressure	Antoine's equation
Density	Ideal gas law (gases, both pure and mixture)
	Modified Rackett's equation (liquids, both pure and mixture)
Molar liquid volume at normal boiling point	Tyn and Calus
Viscosity	Lucas (gases, both pure and mixture)
	Letsou and Stiel (liquids, both pure and mixture)
Thermal conductivity	Chung et al. (pure gases)
	Wassiljewa equation with Mason and Saxena modification (gas mixture)
	Sato-Riedel (pure liquid)
	Li (liquid mixture)
Binary diffusion coefficient	Wilke and Lee (gases)
	Tyn and Calus (liquid binary diffusion coefficient at infinite dilution)
	Taylor and Krishna (liquid binary diffusion coefficient at finite concentration in multi-component mixture)
Mass transfer coefficients	Scheffe and Weiland (for valve tray)
Heat transfer coefficients	Chilton-Colburn analogy

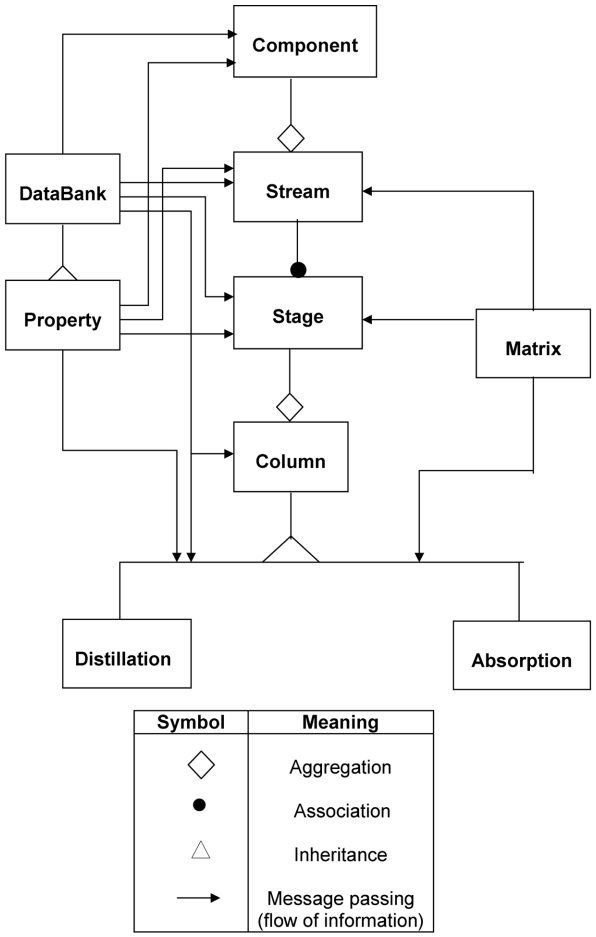

Fig. 2. Object oriented model and nomenclature for a distillation column, with convention based from Rumbaugh et al. [1993].

were generated for the Newton-Raphson scheme by a combination of flash vaporization and bubble point algorithm of Wang and Henke [1966]. Flash calculations, based on the combined feed streams, at an average column pressure and temperature, and specified bottom product flow rate, generated the compositions of vapor and liquid stream products. These were used to estimate the dew point and bubble point temperatures of the vapor and liquid products from the tower. A linear interpolation of these values provided initial estimate of the temperature profile. Initial set of total vapor and liquid flow rates were estimated assuming constant molar inter stage flows by using the specified reflux, distillate, feed, and side-stream flow rates. These estimates from this flash vaporization procedure were improved upon by providing them as initial estimates to the bubble point algorithm. The results after the first few iterations of this algorithm served as the initial guesses for the rate based model solution. The stage temperature so obtained was assigned to bulk liquid and vapor-phases as well as to the interface temperature of the stage. Vapor-liquid interface mole fractions were set to be the same as those of the bulk vapor and liquid stream values. The mass transfer rates (N_{ij}) were all initially assigned to be zero. At this point in the simulation, initial conditions corresponding to equilibrium state of the phases are assumed. The non-ideal solution K-values were used in the above algorithm except for the first iteration when Raoult's law was used.

The highly nonlinear nature of the rate-based model is mainly due to the composition dependency in addition to temperature and pressure of the thermodynamic and physical properties particularly for non-ideal systems. Simulation of extractive distillation processes involves multiple feeds and non-ideal mixtures and hence becomes relatively difficult to converge. The updates to the previous guesses ($\Delta \mathbf{x}$) were scaled by a scalar factor (t) as recommended by Seader and Henley [1998]. A scalar stepping factor (t) was used in order to ensure convergence. When t was taken as unity, implying no modifications of the updates provided by the Newton-Raphson scheme, the simulations failed to converge. But when t was optimized by the golden section method [Cheny and Kincaid, 1999] to a value between 0 and 1 during every iteration of the Newton Raphson scheme, convergence was achieved to yield a feasible solution. During every iteration, optimizing upon the t value minimized the sum of squares of discrepancy functions. In the simulation case study, when t was set to unity, the method failed to converge after 4 iterations. However, using optimal t evaluated during every iteration, a feasible solution was attained in 27 iterations with the specified tolerance.

The initial guess generation procedure involving a combination of flash vaporization and bubble point method did not lead to convergence for the rate based simulations for reflux ratios specified at greater than 7. Hence, an improved version of the application was developed to generate proper initial guesses. Initially, the converged rate based results for a lower reflux ratio were provided as initial guesses. This worked for reflux ratios up to 8. For ensuring convergence at higher reflux ratios, the arc length continuation algorithm as adopted by Vadapalli and Seader [2001] was utilized. Results were found to converge for reflux ratios even as high as 30.

RESULTS AND DISCUSSION

The rate based model simulations of the valve tray column are presented and the interface and bulk values of temperature, vapor and liquid composition are distinguished in Figs. 3a, 4a and 5a. The rate based models results are compared with the Aspen Plus® generated equilibrium model predictions in Figs. 3a, 4b, and 5b. The explanation for the trends shown by the composition profiles is based on King [1980]. Further, the convergence between the equilibrium and rate based model predictions is illustrated when the rate limiting vapor phase mass and heat transfer coefficients were deliberately increased to 10 times their original values in Figs. 3b, 4c and 5c. A thermodynamic analysis indicates the difference between the equilibrium and rate based models. Finally, the design implications of choosing the simple equilibrium model instead of the rigorous rate based model are discussed.

1. Temperature Profiles

It can be observed from the temperature profiles (Fig. 3a) that the liquid bulk and interface temperature profiles are virtually identical but vapor phase temperature profile is different. Hence, the assumption of equality of all temperatures as considered in the equilibrium model is not a good approximation for this system. The interface and liquid temperatures predicted by the rate-based model are almost identical due to negligible resistance to heat transfer in the liquid phase owing to very high liquid phase heat transfer coefficients. The equilibrium model's temperatures are found to be lower

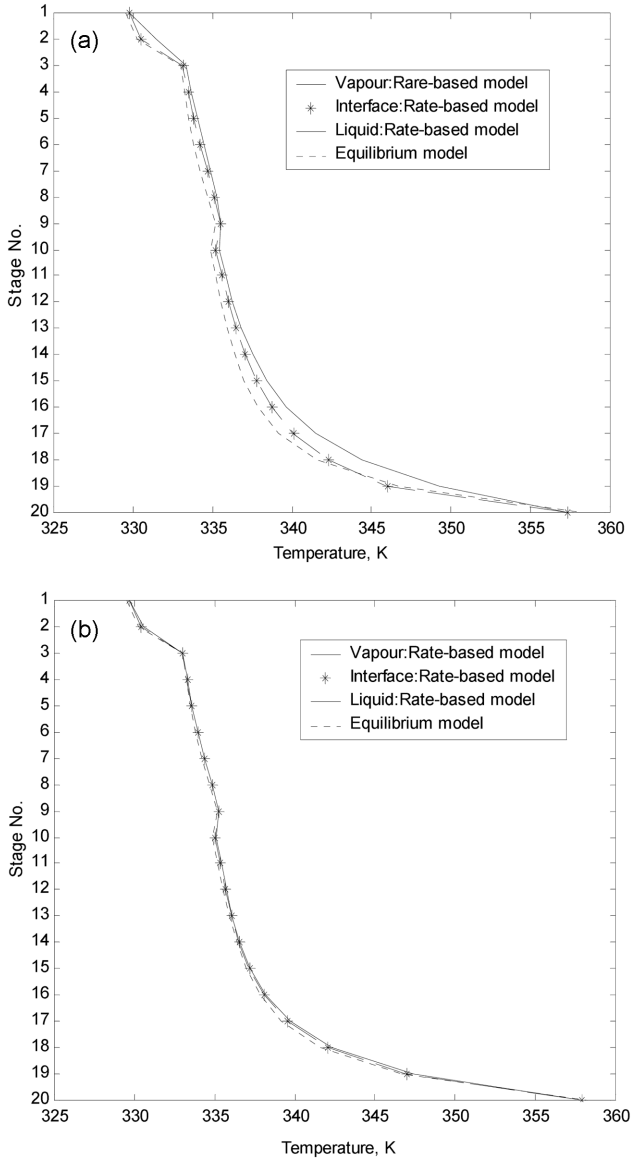

Fig. 3. (a) Rate based model's temperature profiles compared with equilibrium model predictions (Aspen plus®) (b) Temperature profiles upon enhancement of vapor phase mass and heat transfer coefficients.

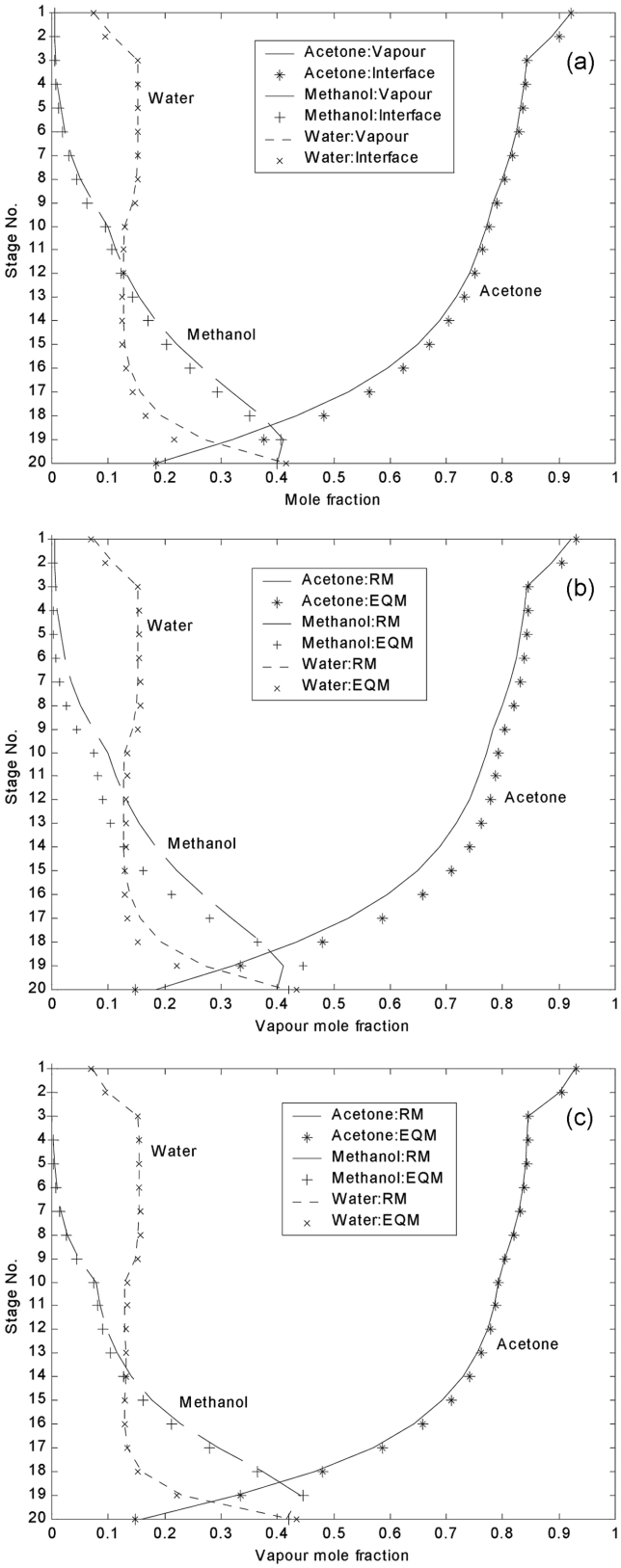

Fig. 4. (a) Vapor phase composition profiles in the bulk and interface from rate-based model, (b) Comparison of bulk vapor phase composition profiles between rate-based model (RM) and equilibrium model (EQM), (c) Effect of increasing vapor phase mass and heat transfer coefficients simultaneously on vapor composition profiles.

than those of the rate-based model's liquid temperatures, which in turn are lower than those of the rate based model's vapor temperatures.

2. Vapor and Liquid Phase Composition Profiles

From Figs. 4 and 5 it is observed that the water concentration decreases very rapidly above stage 3 (zone 1), whereas the acetone concentration increases implying enrichment of acetone in this phase. Between stages 3 to 9 (zone 2), water is present in large quantities and its concentration is almost constant. Methanol gets preferentially absorbed into water and its concentration increases rapidly in this zone. In the lower section of column, i.e., from stages 10 to 20 (zone 3), stripping of acetone from the liquid occurs. Again, water concentration is at a constant but lower concentration up to some stages above the reboiler and then starts increasing rapidly attaining a maximum at the reboiler. The stream from the reboiler is richer in

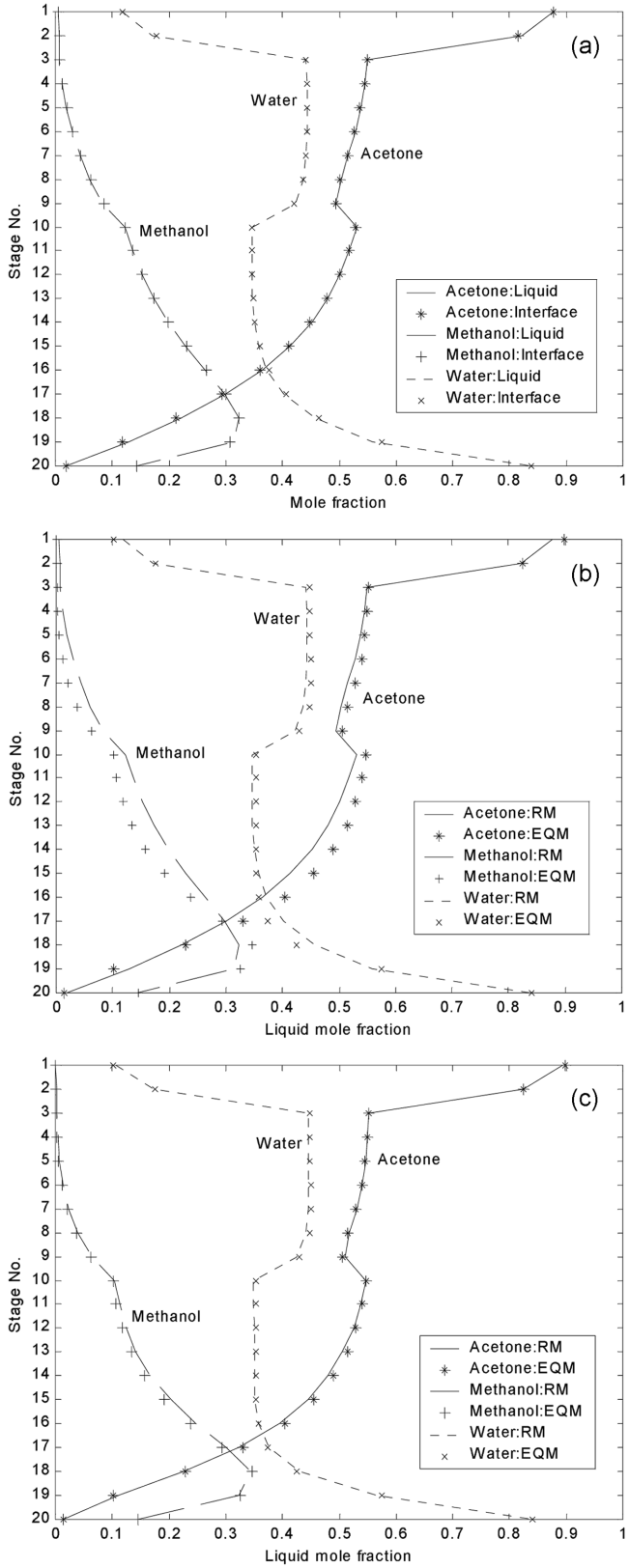

Fig. 5. (a) Liquid phase composition profiles in the bulk and interface from rate-based model, (b) Comparison of bulk liquid phase composition profiles between rate-based model (RM) and equilibrium model (EQM), (c) Effect of increasing vapor phase mass and heat transfer coefficients simultaneously on liquid phase composition profiles.

methanol owing to its relatively higher volatility. However above the reboiler, the methanol is relatively less volatile when compared to acetone, which gets distilled preferentially leading to a hump in the methanol profile.

In the vapor phase, the profiles for the bulk and interface (Fig. 4a) are different implying relatively higher resistance to mass transfer. Significant differences are observed between the bulk vapor phase compositions predicted by rate based and equilibrium models (Fig. 4b). It can be observed that the equilibrium model overpredicts the product purity of acetone in the distillate and underpredicts product impurity of the same component in the residue, implying in both situations higher mass transfer performance of the column than actually observed through the rate based model.

Fig. 5a shows almost identical profiles for the liquid phase bulk and liquid side interface, thereby indicating negligible mass transfer resistance in the liquid phase for this system. However the rate based model predictions again differ from those of the equilibrium model (Fig. 5b).

3. Effect of Mass and Heat Transfer Coefficients

In the present study, the estimated binary mass transfer coefficients in liquid phase were approximately 10 times higher than those in the vapor phase. A typical matrix of multicomponent mass transfer coefficients calculated from film model using the binary mass transfer coefficients given above are as follows:

For Vapor phase

$$k^{V}=\begin{bmatrix} 208.719 & 28.448 \\ 9.701 & 193.321 \end{bmatrix} \quad (1)$$

For Liquid phase

$$k^{L}=\begin{bmatrix} 1334.559 & -114.538 \\ -67.193 & 1323.165 \end{bmatrix} \quad (2)$$

The matrix of high mass flux correction factor was calculated for the present case study to be very nearly the identity matrix as also indicated by Power et al. [1988], and hence neglected in mass transfer rate calculations. Similarly, the heat transfer coefficients in the liquid phase were much higher than those of the vapor phase. To test the sensitivity of the rate based model to the transport coefficients, it was decided to focus on the rate limiting vapor side for the current system.

The vapor phase binary mass transfer coefficients were increased deliberately by ten times the actual value without changing the specifications for the given case study. The other transport coefficient in the same phase, viz., the vapor phase heat transfer coefficient was also correspondingly increased by ten times the actual value. The composition and temperature profiles generated from the rate-based model and equilibrium model simulations are compared for vapor and liquid phases, respectively, in Figs. 3b, 4c and 5c. It can be seen that in both phases, the rate based model compositions and temperatures approach those of the equilibrium model. Comparing Figs. 4a and 4c, it may be observed that as the heat and mass transfer coefficients of the vapor phase are enhanced, the rate based predictions approach the equilibrium model. Owing to closer approach to equilibrium, the impurity of acetone in the bottom stream has reduced considerably from 0.184 to 0.159.

4. Thermodynamic Analysis

The effects of composition and temperature in the various phases were combined in terms of the thermodynamic parameter fugacity in order to illustrate the differences between the rate based and equilibrium model. At equilibrium fugacity of species i (f_i) in both vapour and liquid mixture should be equal, i.e.,

$$f_i^V = f_i^L \tag{3}$$

Fugacity of species i in vapour (f_i^V) and liquid (f_i^L) mixture can be calculated as follows:

$$f_i^V = \phi_{iv} y_i P \tag{4}$$

$$f_i^L = \phi_{il} x_i P \tag{5}$$

Component fugacities in both vapour and liquid mixtures for all stages are plotted in Fig. 6 for the original simulation and in Fig. 7

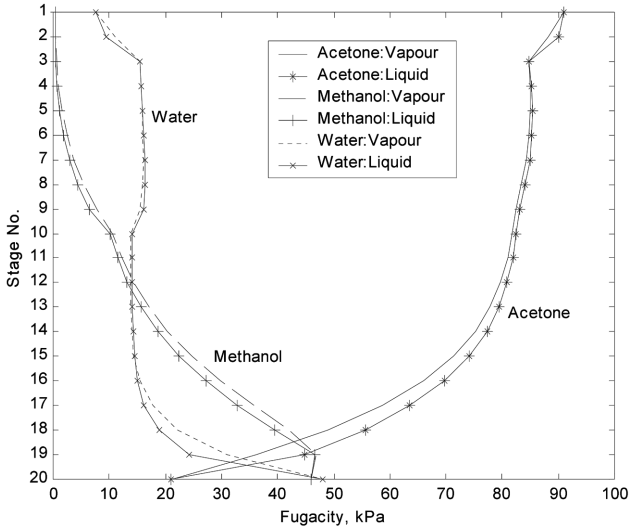

Fig. 6. Component fugacities in vapour and liquid phase for rate-based model simulation.

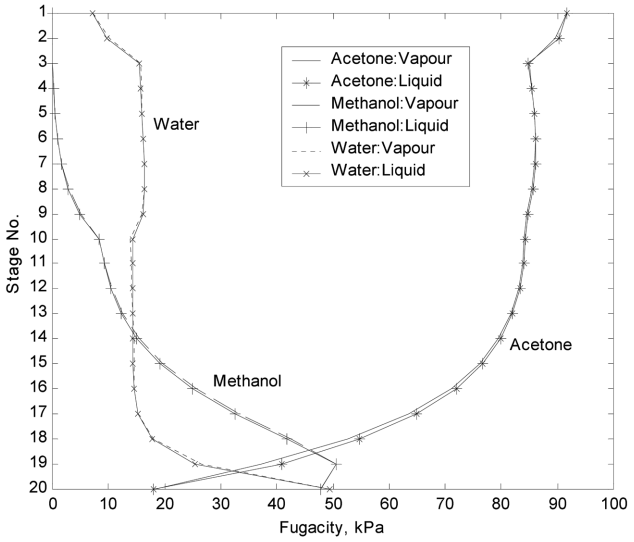

Fig. 7. Effect of increasing vapor phase mass and heat transfer coefficients simultaneously on component fugacities.

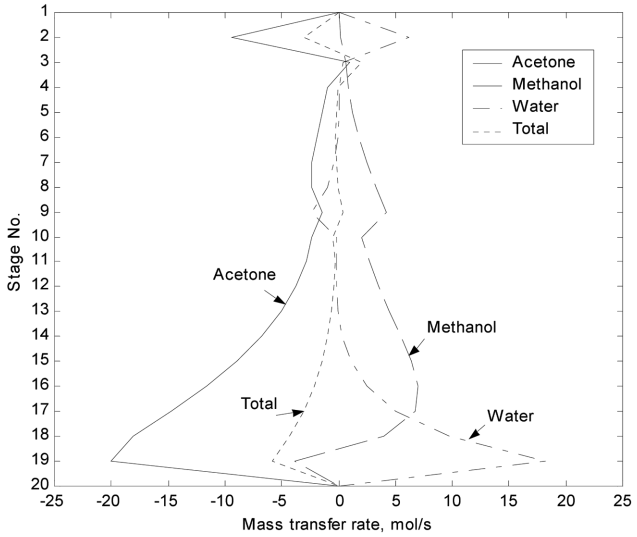

Fig. 8. Mass transfer rate profiles.

for simulations carried out with enhanced mass and heat transfer coefficients. Differences between the vapor and liquid phase fugacities can be observed for each component in most of the stages. Upon simultaneous increase in mass and heat transfer coefficients, the vapor and liquid phase fugacity profiles for each component approach one another.

5. Mass Transfer Rates

The inter-phase molar transfer rate for individual components (N_{ij}) and total inter-phase molar transfer rate (N_T) are plotted from the rate-based model simulation (Fig. 8). The signs for the individual mass transfer rates are dictated by the values of the compositions at the bulk relative to the interface. The profiles indicate that the total molar transfer rate is not negligible everywhere in the column. Hence the commonly made assumption of equimolar counter diffusion for multicomponent distillation is not applicable here. It can be seen that the mass transfer rate for acetone and water is found to be relatively higher than methanol in zone 1. The negative mass transfer rates of acetone indicate the transfer of acetone from liquid to vapor. This suggests that at the top section separation occurs mostly between acetone and water as discussed previously. In zone 2, the component mass transfer rates for acetone and methanol are higher when compared to water. Further, the signs of the mass transfer rates of the two components are different, implying transfer in opposite directions. In zone 3, the mass transfer of acetone occurs at a higher rate from liquid to vapor, indicating vigorous stripping of acetone from the mixture. The transfer rate of water, the least volatile substance is relatively higher on stages just above the reboiler and occurs from vapor to liquid as expected. In this section above the reboiler, methanol also transfers from vapor to liquid. These phenomena are consistent with composition profiles.

DESIGN IMPLICATIONS OF THE RATE BASED MODEL

When the mass transfer coefficients are very high, the predictions of rate-based model simulating a real column approaches that of the equilibrium stage model. Hence, to achieve higher mass trans-

Table 7. Comparison of product purities predicted by the rate based and equilibrium models for the case study discussed

Number of stages	Solvent stage location	Feed stage location	Purity of acetone (mole fraction) in the vapor distillate	Impurity of acetone (mole fraction) in the liquid residue	Mole fraction of methanol in vapor distillate	Mole fraction of methanol in liquid residue
Rate based model						
20	3	10	0.9212	0.01793	0.0039	0.1436
Equilibrium model						
20	3	10	0.93008	0.0139	0.00042	0.1452
16	3	8	0.92907	0.0143	0.00214	0.1444
12	3	6	0.92298	0.0171	0.0117	0.1400
10	3	5	0.91408	0.0211	0.02531	0.1339

fer performance the tray design assumes significance. Other conclusions important from the design viewpoint are discussed below.

1. Product Compositions

From the composition profiles (Figs. 4 and 5) it has been observed that the equilibrium stage model over-predicts the column performance in terms of acetone purity achieved in distillate and acetone impurity left over in the residue. The product purities attained in the rate based and equilibrium models are tabulated in Table 7 for acetone and methanol. Only stages lower than 20 were tried as the equilibrium model with 20 stages performed better than the rate based model. The feed stage location was varied according to the numbers of stages, while the solvent feed stage was fixed at the third tray. The other specifications like feed flow rate, temperature and pressure, solvent flow rate, temperature and pressure, reflux ratio, bottom rate were the same as before. Though the difference in product purities does not seem to be much, the number of stages required by the equilibrium model to attain close to the acetone distillate composition of 0.921 predicted by the rate based model is only 60% of those required by the rate based model. Though efficiencies can be used to account the deviation from non-ideality, prediction of efficiency is not reliable always as it can be very sensitive to composition, vary from one component to another as well as from one stage to the next, and can be even unbounded. The Murphree efficiencies back calculated from the present case study are shown in Fig. 9.

2. Feed Stage Location

Locations of the feed stages have a significant influence on the purity of the product streams. Several simulations were carried out to find the most suitable combination of the solvent and feed stage locations that will maximize the purity of acetone in the distillate while maintaining the total number of stages at 20. As can be seen from Table 8, the optimum feed and solvent stage locations from the equilibrium model was estimated to be 4 and 14, respectively, while the corresponding rate based model predicted them to be at 4 and 11. Further, the discrepancies in the acetone purities of the distillate stream can also be noted.

Table 8. Comparison of optimum feed and solvent stage locations of rate based and equilibrium models for the case study discussed

Parameter	Equilibrium model	Rate based model
Most suitable solvent stage location	4	4
Most suitable feed stage location	14	11
Acetone purity in distillate	0.9424	0.9312

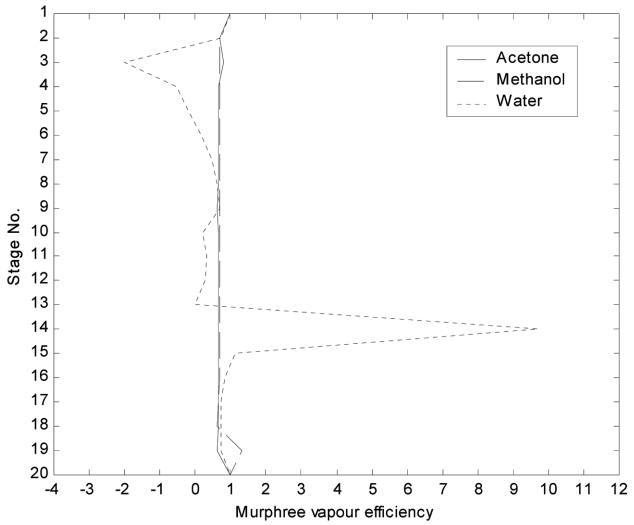

Fig. 9. Murphree vapor efficiency profile back calculated from rate-based model simulation.

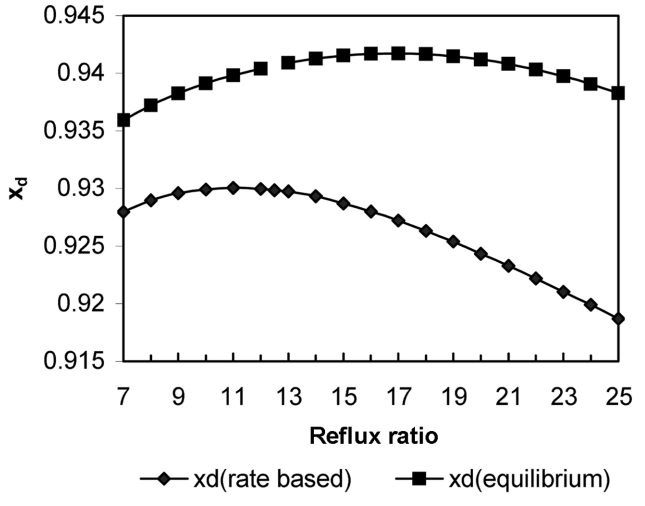

Fig. 10. Comparison of effect of reflux ratio between rate based and equilibrium stage models. Equilibrium stage model predictions are from Aspen Plus®.

3. Effect of Reflux Ratio

A surprising effect of reflux ratio on the acetone purity in the distillate was noticed for the extractive distillation process. After a critical reflux ratio that was different for the rate based and equilibrium stage models, the acetone product purity was actually found to decrease. This can be explained by the conflicting effects of the positive action of reflux versus the reduction in relative volatility between azeotropic constituents at increasing reflux ratios. This translates in terms of the effect of water flow rate on the activity coefficients of acetone and methanol. The activity coefficient of acetone increases with increasing water flow rates leading to enhancement in the relative volatility of acetone-methanol pair. However, at increasing reflux the enriching action has to be balanced against the diluting effect of the (water lean) reflux stream on the water composition and consequently its capability to improve the relative volatility. Since the compositions and temperatures are different between the rate based and equilibrium staged model, it is to be expected that the critical reflux ratios would be different between the two model predictions as well. The effect of reflux ratio is shown in Fg. 10.

CONCLUSIONS

The rigorous simulation of a valve tray column through the rate based approach provided several useful results. The rate-based model, though complicated relative to the equilibrium model, provides a realistic estimate of the distillation column performance without incorporating efficiency factors. When the mass and heat transfer coefficients are high, the rate based model predictions approaches that of the equilibrium model predictions. High mass and heat transfer rates can be achieved by improving upon the tray design so that the actual column performs closest to that of an ideal column. The purity of acetone in the distillate predicted by the rate based model is significantly lower than that predicted by the equilibrium stage model. Equivalently, the equilibrium model requires far fewer stages to attain the distillate composition of the rate-based model. Further, there were significant differences between the two models in predicting the most suitable location of the feed entry. The counter-intuitive and counter-productive effect of reflux ratio on separation is explained. Experimental data on extractive distillation in valve tray columns are recommended to support rigorous mathematical modeling studies as well as to identify optimal operating conditions and design parameters.

ACKNOWLEDGMENT

This work was partly supported by the All India Council for Technical Education (AICTE) through the scheme of CAYT to the corresponding author. A part of this work was presented at the "National Conference on Separation in Process Industries" held at Institute of Technology, Varanasi-221 005, India on February, 14-16, 2003.

NOMENCLATURE

a : interfacial area per unit active area
d : characteristic length, taken as 1 m
D : diffusion coefficient [$m^2 \cdot s^{-1}$]
E_{MV} : Murphree tray efficiency
f_{ij}^L : liquid feed flow rate of species i to stage j [mol/s]
f_{ij}^V : vapor feed flow rate of species i to stage j [mol/s]
F_j : total vapor feed flow rate to stage j [mol/s]
F_j^L : total liquid feed flow rate to stage j [mol/s]
F_j^V : total vapor feed flow rate to stage j [mol/s]
G : superficial gas mass velocity [$kg \cdot m^{-2} \cdot s^{-1}$]
H_j^L : enthalpy of liquid stream leaving stage j [J/mol]
H_j^{LF} : enthalpy of liquid feed stream entering to stage j [J/mol]
H_j^V : enthalpy of vapor stream leaving stage j [J/mol]
H_j^{VF} : enthalpy of vapor feed stream entering to stage j [J/mol]
$k_x a$: liquid-side mass-transfer coefficient based on mole fraction driving force [kg-mol $\cdot m^{-2} \cdot s^{-1}$]
$k_y a$: gas-side mass-transfer coefficient based on mole fraction driving force [kg-mol $\cdot m^{-2} \cdot s^{-1}$]
L : superficial liquid mass velocity [$kg \cdot m^{-2} \cdot s^{-1}$]
L_j : inter-stage total liquid flow rate from stage j [mol/s]
M : molecular weight
N_{ij} : inter-phase mass transfer rate of species 'i' in stage 'j' [mol/s]
P : total pressure [kPa]
Q_j : external heat transfer to or from the stage j [J/s (Watt)]
Q_j^L : external heat transfer to or from the stage j in liquid phase [J/s (Watt)]
Q_j^V : external heat transfer to or from the stage j in vapour phase [J/s (Watt)]
r_j^L : fraction of the liquid exiting the stage j withdrawn as liquid side stream [U_j/L_j]
r_j^V : fraction of the vapor exiting the stage j withdrawn as vapor side stream [W_j/V_j]
Re_G : gas-phase Reynolds number=Gd/μ_G
Re_L : gas-phase Reynolds number=Ld/μ_L
Sc_G : Schmidt number in gas-phase= ν_G/D_G
Sc_L : Schmidt number in gas-phase= ν_L/D_L
Sh_G : gas-side Sherwood number=$k_y ad/\rho_G D_G$
Sh_L : gas-side Sherwood number=$k_x ad/\rho_L D_L$
T : temperature [K]
U_j : liquid side stream flow rate from stage j [mol/s]
V_i : molar volume of the pure liquid of species [$kmol/m^3$]
V_j : interstage total vapor flow rate from stage j [mol/s]
W : weir height [m]
W′ : dimensionless weir height=W/d
W_j : liquid side stream flow rate from stage j [mol/s]
x_i : mole fraction, liquid
y_i : mole fraction, gas

Greek Letters

μ : viscosity in Re [$kg \cdot m^{-1} \cdot s^{-1}$]
ρ : bulk-phase molar density [kg-mol $\cdot m^{-3}$]
ϕ_i : fugacity coefficient of species i
γ_i : activity coefficient of species i
δ_{ij} : Kronecker delta, 1 if i=j, 0 if i≠j

Superscripts

V : vapor phase
L : liquid phase
I : interface

Subscripts

V : vapor phase
L : liquid phase
I : interface

REFERENCES

Aspen Plus® Steady State Simulation Version 10.1-0, Aspen Technology Inc.

Assabumrungrat, S., Wongwattanasate, D., Pavarajarn, V., Praserthdam, P., Arpornwichanop, A. and Goto, S., "Production of Ethyl *tert*-Butyl Ether from *tert*-Butyl Alcohol and Ethanol Catalyzed by *β*-Zeolite in Reactive Distillation," *Korean J. Chem. Eng.*, **21**(6), 1139 (2004).

Cheny, W. and Kincaid, D., *Numerical Mathematics and Computing*, 4th ed., Brooks/Cole Publishing Co., USA (1999).

Higler, A., Chande, R., Taylor, R., Baur, R. and Krishna, R., "Non-Equilibrium Modeling of Three-Phase Distillation," *Comp. and Chem. Eng.*, **28**, 2021 (2004).

Hoffmann, A., Noeres, C. and Górak, A., "Scale-Up of Reactive Distillation Columns with Catalytic Packings," *Chem. Eng. Process*, **43**, 383 (2004).

Kenig, E. Y., Gorak, A., Pyhalahti, A., Jakobsson, K., Aittamaa, J. and Sundmacher, K., "Advanced Rate-Based Simulation Tool for Reactive Distillation," *AIChE J.*, **50**, 322 (2004).

Kim, Y. H., Hwang, K. S. and Nakaiwa, M., "Design of a Fully Thermally Coupled Distillation Column For a Hexane Process Using a Semi-Rigorous Model," *Korean. J.Chem. Eng.*, **21**, 1098 (2004).

King, C. J., *Separation Processes*, McGraw-Hill Book Company, New York (1980.)

Kister, H. Z., *Distillation Design*, McGraw Hill, New York (1992).

Kloker, M., Kenig, E. Y., Schmitt, M., Althaus, K., Schoemakers, H., Markusse, P. and Kwant, G, "Influence of Operating Conditions and Column Configuration on the Performance of Reactive Distillation Columns with Liquid-Liquid Separators," *Can. J Chem Engg*, **81**, 725 (2003).

Lee, Y. S., Kim, M. G and Ha, D. M., "Analysis of Packed Distillation Columns With a Rate Based Model," *Korean J. Chem. Eng.*, **14**, 321 (1997).

Mortaheb, H. R. and Kosuge, H., "Simulation and Optimization of Heterogeneous Azeotropic Distillation Process with a Rate-Based Model," *Chem. Eng. Process*, **43**, 317 (2004).

Noeres, C., Dadhe, K., Gesthuisen, R., Engell, S. and Górak, A., "Model-Based Design, Control and Optimization of Catalytic Distillation Processes," *Chem. Eng. Process*, **43**, 421 (2004).

Peng, J., Edgar, T. F. and Eldridge, R. B., "Dynamic Rate-Based and Equilibrium Models for a Packed Reactive Distillation Column," *Chem. Eng. Sci.*, **58**, 2671 (2003).

Powers, M. F., Vickery, D. J., Arehole, R. and Taylor, R., "A Nonequilibrium Stage Model of Multi-component Separation Processes: V. Computational Methods for Solving the Model Equations," *Comput. & Chem. Engg.*, **12**, 1229 (1988).

Pyhalahti, A. and Jakobsson, K., "Rate-based Mixed-Pool Model of a Reactive Distillation Column," *Ind. Eng. Chem. Res.*, **42**, 6188 (2003).

Reid, R. C., Prausnitz, J. M. and Poling, B. E., *The Properties of Gases and Liquids*, 4th ed., McGraw-Hill, New York (1988).

Rumbaugh, J., Blaha, M., Premerlani, W., Eddy, F. and Lorensen, W., *Object-Oriented Modeling and Design*, Prentice-Hall of India, New Delhi (1997).

Sanpui, D. and Khanna, A., "Selection of Mass Transfer Correlations for Rate Based Liquid-Liquid Extraction Model," *Korean J. Chem. Eng.*, **20**, 609 (2003).

Seader, E. J. and Henley, J. D., *Separation Process Principles*, John Wiley, Singapore (1998).

Scheffe, R. D. and Weiland, R. H., "Mass Transfer Characteristics of Valve Trays," *Ind. Eng. Chem. Res.*, **26**, 228 (1987).

Springer, P. A. M., Van Der Molen, S. and. Krishna, R., "The Need for Using Rigorous rate-Based Models for Simulations of Ternary Azeotropic Distillation," *Comp. and Chem. Eng.*, **26**, 1265 (2002).

Taylor, R. and Krishna, R., *Multi-component Mass Transfer*, John Wiley & Sons, Inc., New York (1993).

Toor, H. L., "Diffusion in Three Component Gas Mixtures," *AIChE J.*, **3**, 198 (1957).

Toor, H. L., "Prediction of Efficiencies and Mass Transfer on a Stage with Multicomponent Systems," *AIChE J.*, **10**, 545 (1964).

Vadapalli, A. and Seader, J. D., "A Generalized Framework for Computing Bifurcation Diagrams Using Process Simulation Programs," *Comp. Chem. Engg.*, **25**, 445 (2001).

Wang. J. C and Henke, G. E., "Tridiagonal Matrix for Absorbers?," *Hydrocarbon Processing*, **45**(8), 155 (1966).